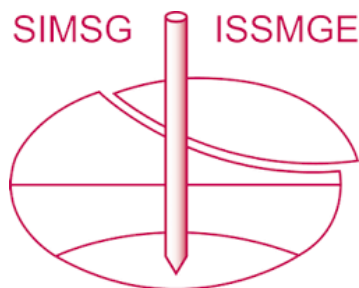


# INTERNATIONAL SOCIETY FOR SOIL MECHANICS AND GEOTECHNICAL ENGINEERING



*This paper was downloaded from the Online Library of the International Society for Soil Mechanics and Geotechnical Engineering (ISSMGE). The library is available here:*

<https://www.issmge.org/publications/online-library>

*This is an open-access database that archives thousands of papers published under the Auspices of the ISSMGE and maintained by the Innovation and Development Committee of ISSMGE.*

*The paper was published in the Proceedings of the 8<sup>th</sup> International Symposium on Deformation Characteristics of Geomaterials (IS-PORTO 2023) and was edited by António Viana da Fonseca and Cristiana Ferreira. The symposium was held from the 3<sup>rd</sup> to the 6<sup>th</sup> of September 2023 in Porto, Portugal.*

# An automated system for determining soil parameters: Case study

Islam Marzouk<sup>1#</sup>, Simon Oberhollenzer<sup>1</sup>, and Franz Tschuchnigg<sup>1</sup>

<sup>1</sup>Graz University of Technology, Graz, Austria

<sup>#</sup>Corresponding author: islam.marzouk@tugraz.at

## ABSTRACT

The success of numerical analysis depends on several factors. One of the key factors is the accurate determination of constitutive model parameters. Determining these parameters from in-situ tests has several advantages compared to laboratory tests, from lower costs to minimal disturbance of the soil. However, it is not possible to derive soil parameters directly from in-situ test results, since correlations are required. The literature offers a wide range of correlations which increases the uncertainty during interpretation. The ongoing research project APD (Automated Parameter Determination) investigates the possibilities of automated parameter identification from in-situ tests using a graph-based approach. In the present paper, existing correlations – developed for cone penetration tests – are validated by comparing their output to laboratory results. The Norwegian GeoTest Sites (NGTS) infrastructure project consists of five test sites in different soils in Norway. The data from the soft clay site located in Onsøy, south-eastern Norway was used in the validation process. A web-based application “Datamap” that has been developed to capture, organize, and classify geotechnical research data has been used to obtain in-situ and laboratory test data. The further validation of existing correlations to derive accurate constitutive parameters from in-situ tests is part of ongoing research.

**Keywords:** automated parameter determination; in-situ testing; graph theory; soil parameters.

## 1. Introduction

Numerical analysis has several advantages over traditional methods, mainly in the level of insight that can be obtained in several geotechnical engineering problems such as soil-structure interaction (Brinkgreve 2019). The success of numerical analyses is influenced by several aspects. One of the most important aspects lies in the determination of the constitutive model parameters. It is often the case that these parameters need to be assessed based on laboratory tests (e.g., triaxial and oedometer tests) which are not always available in all projects.

As an alternative, the cone penetration test (CPT) is a widely used in-situ test in geotechnical engineering for soil profiling and soil parameters determination. The latter in-situ test is fast and cheaper compared to laboratory testing and introduces a small disturbance during test execution. However, it is not possible to derive soil parameters directly from in-situ measurements (tip resistance  $q_c$ , sleeve friction  $f_s$ ). Several empirical correlations have been proposed in the literature to link soil parameters with in-situ measurements. Since various correlations have been developed for the same parameter, a significant scatter can be obtained when comparing the obtained results. The reason for this scatter lies mainly in the applicability of individual correlations (e.g. correlations only suitable for specific soil types). There are several guides available dealing with the interpretation of CPT such as (Kulhawy and Mayne 1990; Lunne, Robertson, and Powell 1997; Mayne 2014; Robertson 2015).

An ongoing research project aims to create an automated parameter determination (APD) system to determine constitutive model parameters based on in-situ tests. The system is based on a graph-based approach which inherits some of the characteristics of graph theory (van Berkomp et al. 2022). It is the aim of the project to create a parameter determination framework characterized by transparency and adaptability. The former is achieved by describing how the available information is used to determine parameters and the latter is ensured by allowing the users to integrate their knowledge and experience into the system.

van Berkomp et al. (2022) illustrated the framework and described the determination of parameters for coarse-grained soils. Marzouk et al. (2022) extended the framework by determining parameters for fine-grained soils. This paper presents a case study where this framework is used to determine soil parameters and the outcome is compared to reference values (laboratory test data). The case study is based on one of the Norwegian GeoTest Sites (NGTS), namely Onsøy soft clay site.

## 2. Norwegian GeoTest Sites (NGTS) – Onsøy soft clay

### 2.1. Datamap

“Datamap” is a novel web application that has been developed to capture, classify and organize geotechnical data. It provides a general platform for making geotechnical data available and allows researchers to create and share their projects. The web application can

be accessed through [www.geocalcs.com/datamap](http://www.geocalcs.com/datamap) (Doherty et al. 2018).

## 2.2. Norwegian GeoTest Sites (NGTS)

Five GeoTest Sites (NGTS) have been established in Norway between 2016 and 2019 by the Norwegian Geotechnical Institute (NGI), the Norwegian University of Science and Technology (NTNU), SINTEF Building and Infrastructure, the University Centre in Svalbard (UNIS), and the Norwegian Public Roads Administration (NPRA) (L'Heureux and Lunne 2020). The five sites correspond to different soil types (clay, silt, quick clay, sand and permafrost).

## 2.3. Onsøy soft clay

The NGTS soft clay site at Onsøy was established in 2016 and has a potential testing area of approximately  $80 \text{ m} \times 75 \text{ m}$ . An extensive laboratory and field testing program has been conducted and is presented in NGI's report (Norwegian Geotechnical Institute 2019). In-situ testing consisted of cone penetration tests (CPT), seismic cone penetration tests (SCPT), seismic flat dilatometer test (SDMT) and self-boring pressuremeter test (SBP). Laboratory testing included the determination of in-situ water content, unit weight, Atterberg limits and the execution of constant rate of strain oedometer tests (CRS), triaxial tests, direct simple shear tests (DSS), where block and different types of tube samplers were used for sample recovery (Gundersen et al. 2019).

There were two main areas of investigation, south-central (SC) and southeast corner (SEC). The stratigraphy of the test site consisted of 4 main units which are slightly overconsolidated (Gundersen et al. 2019). Unit I consists of weathered clay. Unit II is described as a clay of high to very high plasticity index ( $PI \approx 44\%$ ). Unit III is identified as clay of medium high plasticity index ( $PI \approx 27\%$ ). Unit IV has similar index properties as Unit II; however, the plasticity index, water content and clay content decrease towards the bedrock.

The thickness of these units is different with respect to the two investigation areas (SC & SEC). The thickness of Unit I is 1 m in both areas. While for Unit II, the thickness is around 7 m and 9.5 m for areas SC and SEC respectively. The thickness of Unit III is equal to 5.5 m at (SC) area and 9 m at (SEC) area (Gundersen et al. 2019).

In this study, CPTu 2 (executed in area SC) and CPTu 18 (executed in area SEC) are selected for discussion (CPTu 2 and CPTu 18 correspond to ONSC02 and ONSC18 respectively in the database uploaded at Datamap). Fig. 1 shows the in-situ measurements for CPTu 2 and CPTu 18 and the boundaries between individual units. The boundaries of area SC are represented by the black dotted horizontal lines in subplot  $q_c$ , while for SEC, the boundaries are represented by the blue dotted horizontal lines in subplot  $u_2$ . CPTu 2 had a different rate of penetration (12 mm/s) compared to CPTu 18 (20 mm/s). As CPTu 2 was the only CPT carried out in area SC, it was selected as the representative CPT for this area. The two CPTs were used in the APD system to determine soil parameters and the obtained values

were compared with laboratory results. The groundwater level was located 1 m below the ground surface during test execution.

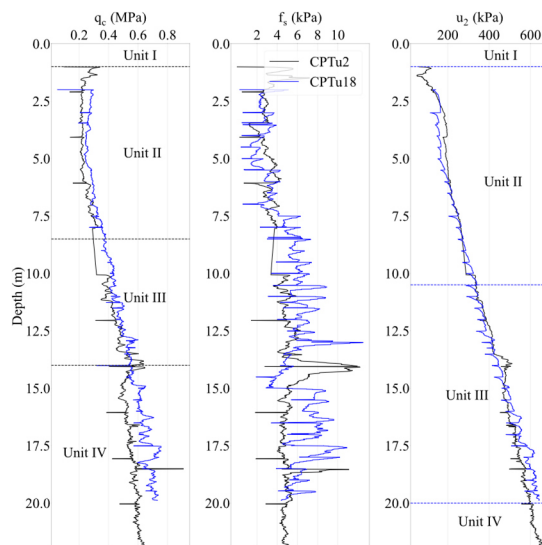


Figure 1. Overview of in-situ measurements for CPTu 2 and CPTu 18.

## 3. Automated Parameter Determination framework

The automated parameter determination system is built in the programming language Python. The framework consists of several modules as shown in Fig. 2. In the 1<sup>st</sup> module (GEF reader), CPTu raw data is imported in Geotechnical Exchange Format (GEF). Afterwards, CPT(u) measurements (cone resistance  $q_c$ , sleeve friction  $f_s$  & porewater pressure readings  $u_2$ ) are transferred to the 2<sup>nd</sup> module (CPT layer interpretation). The soil behaviour type (SBT) is determined according to one of the following three charts:

- Robertson's normalized SBT chart (Robertson 2009)
- Robertson's modified non-normalized SBT chart (Robertson 2010)
- Robertson's updated normalized SBT chart (Robertson 2016)

In the next step, the CPT profile is stratified into several layers sharing the same SBT. The stratification is done either by one of implemented stratification algorithms or manually by the user of the system. Stratification algorithms are out of scope of this paper and the stratification was assigned manually for this study (see section 5).

After determining the layers, in-situ measurements (cone resistance  $q_c$ , sleeve friction  $f_s$  & porewater pressure readings  $u_2$ ) are averaged within individual layers for parameter identification (e.g., for a layer between -2 m and 5 m below the ground surface, the CPT measurements between these two depths are averaged).

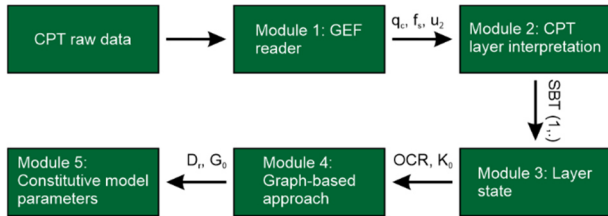
The averaged CPT measurements for each layer are used by module 3 (Layer state) to compute the state (overconsolidation ratio  $OCR$  and coefficient of earth pressure  $K_0$ ) of each layer. The output of the 2<sup>nd</sup> and 3<sup>rd</sup> modules is transferred to module 4 (Graph-based approach). In this module, soil parameters are computed

**Table 1.** Method CSV file format

Method to	Formula	parameters in	parameters out	validity	Reference
method_to_K0	$1 - \sin(\varphi')$	$\varphi'$	K0	SBT(1234567)	Jaky_1944

based on correlations, selected by the user. Module 5 (Constitutive model parameters) uses the parameters obtained in module 4 to calculate constitutive model parameters.

In this paper, the output of module 4 (soil parameters) is presented. The transition to constitutive model parameters (module 5) is not considered.

**Figure 2.** Overview of modules, used for automated parameter determination.

### 3.1. Graph-based approach

The graph-based approach implemented in APD is illustrated in detail in van Berkom et al. (2022). Fig. 3 summarizes the basic concept: source parameters (CPT raw data) are linked to destination parameters (soil or constitutive model parameters) via intermediate parameters. This is achieved based on a given set of correlations. The system creates all paths (chains of correlations) that link source parameters to destination parameters. In addition, it computes the value(s) of the destination parameters.

Within the framework of APD, the terms ‘correlation’, ‘formula’, ‘equation’, ‘rule of thumb’ are replaced by the term ‘method’. It was decided to use this general term as there are several ways to determine parameters (e.g., tables or charts) (van Berkom et al. 2022).

The system automatically links the methods and parameters sharing a relationship. A method to calculate the coefficient of earth pressure at rest is used as an illustrative example. The method according to Jaky (1944) is defined as follows,  $K_0 = 1 - \sin(\varphi')$ , where  $K_0$  is the coefficient of earth pressure at rest and  $\varphi'$ , is the effective friction angle of the soil. The input and the output for this method ( $\varphi'$  and  $K_0$  respectively) must be identified by the system. As a result, links connecting these parameters must be generated.

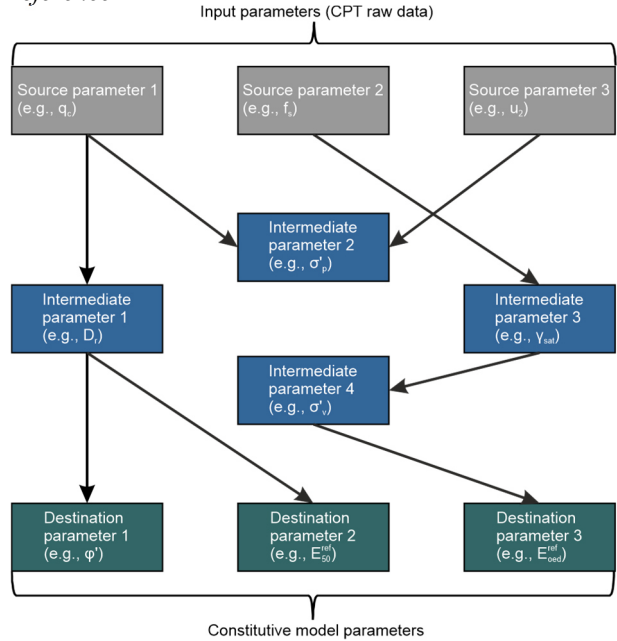
### 3.2. Generating the graph

The output and input(s) of different methods define the relationships between methods and parameters. Consequently, methods and parameters are considered as external inputs to the system. Methods and parameters are defined in separate spreadsheets in comma-separated values (CSV).

These two files (corresponding to methods and parameters) are imported by the system. A standard database of methods and parameters is provided alongside the system. The current version of APD

contains more than 100 methods. Nevertheless, users could extend or modify the standard database. Using the two CSV files, the system creates links connecting methods and parameters, and calculates the value(s) of intermediate and destination parameters.

The two CSV files need to be defined based on a template. Each column in the file correspond to a special property that needs to be specified as follows: *method\_to*, *formula*, *parameters\_in*, *parameters\_out*, *validity* and *reference*.

**Figure 3.** Graph-based approach implemented in APD.

Once more using the method of coefficient of earth pressure at rest as an illustrative example, the entries for this method are shown in Table 1. In the field of *method\_to*, the name of the method is stated (e.g., method\_to\_K0 as shown in Table 1). *formula* presents the equation which is used to compute the output (e.g.,  $1 - \sin(\varphi')$  as shown in Table 1). *parameters\_in* and *parameters\_out* specify the input(s) and the output of this method, respectively. The *validity* field defines the applicability of the methods. As some methods are applicable for all types of soils, other methods are restricted to either coarse-grained or fine-grained soils (or have other limitations). The *validity* is based on the modified non-normalized Robertson’s charts, described in section 3 (Robertson 2010). The *validity* for methods should be defined according to Table 2, by defining the respective number(s). In case the method is only valid for silts, the validity should be set to SBT(4). The method for deriving  $K_0$  is valid for different soil types, the validity is set to SBT(1234567), as shown in Table 1. Finally, in the field of *reference*, the author of the method can optionally be stated (e.g., Jaky\_1944).

Parameters that have been used in the methods CSV file (in the fields of *parameters\_in* and *parameters\_out*) must be defined in the parameters CSV file. The parameters CSV file requires the definition of the

following properties, *symbol*, *value*, *unit*, *constraints* and *description*. In the *symbol* field, the notation of the parameter (similar to the notation used in the method CSV file) is stated (e.g., K0 for the coefficient of earth pressure at rest). The *value* field defines a certain value for the parameter. This value can be specified manually by the user (e.g., unit weight of water), otherwise it should remain empty as the value is calculated by the system. The *unit* field is an optional field where the user can define the unit of the parameter. It is recommended to specify the unit for all parameters to avoid mistakes due to unit conversions. The *constraints* field is another optional argument that applies lower and upper bounds to respective parameters. In case the system calculates a value for this specific parameter higher than the upper bound or lower than the lower bound, this value will be discarded. Finally, in the field of *description*, the user could describe the parameter (e.g., K0 is the coefficient of earth pressure at rest).

**Table 2.** Definition of SBT according to Robertson (2010)

Zone	Soil Behaviour Type (SBT)
1	Sensitive fine-grained
2	Clays – organic soil
3	Clays: clay to silty clay
4	Silt mixtures: clayey silt & silty clay
5	Sand mixtures: silty sand to sandy silt
6	Sands: clean sands to silty sands
7	Dense sand to gravelly sand
8	Stiff sand to clayey sand (overconsolidated)
9	Stiff fine-grained (overconsolidated)

The system imports the two CSV files (methods and parameters) and creates the respective connections between methods and parameters. Subsequently, a graph presenting the links between parameters and the methods is generated. As shown exemplarily in Fig. 4, the computed value(s) for all parameters are summarized in the graph.

#### 4. CPT interpretation

The standard database of methods and parameters provided alongside APD is continuously updated and improved. It consists of more than 100 methods. Nonetheless, users of the system are responsible for validating the output of the system, even if the provided standard database is used. Users would still need to apply their knowledge and experience to the outcome of the system. Nevertheless, with limited experience in geotechnical engineering, the system should provide reliable values for parameters.

In this paper, the graphs are generated based on a selected (limited) number of methods. The selected methods are presented in the following subsections.

##### 4.1. Initial parameters

An initial estimation of the unit weight is required to compute the total ( $\sigma_v$ ) and effective ( $\sigma'_v$ ) stresses, which are further required to estimate CPT parameters (e.g., normalized cone resistance). Therefore, the in-situ unit weight needs to be assessed in the first stage. This initial

unit weight can be calculated using one of the following two equations:

$$\gamma_t = \gamma_w [0.27(\log R_f) + 0.36(\log q_t/p_a) + 1.236] \quad (1)$$

by (Robertson and Cabal 2010), where  $\gamma_w$  is the unit weight of water,  $p_a$  is the atmospheric pressure,  $R_f$  is the friction ratio ( $R_f = f_s/q_c$  100%) and  $q_t$  is the corrected cone resistance, defined as  $q_t = q_c + (1 - a) \times u_2$ , where  $a$  is the cone tip net area ratio.

$$\gamma_t = 19 - 4.12 \left[ \frac{\log(\frac{5}{q_t})}{\log(\frac{36}{R_f})} \right] \quad (2)$$

by (Lengkeek, Greef, and Joosten 2018).

Other methods (correlations) could be used as well to compute the initial unit weight, such as:

$$\gamma_t = 26 - \frac{14}{1 + [0.5 \log f_s + 1]^2} \quad (3)$$

by (Mayne 2014).

In this study, Eq. (2) was used to assess the initial unit weight (which is used to compute the total and effective stresses), since a better agreement with laboratory results was reached (see section 5). A comparison between these 3 methods (Eqs. 1-3) is provided in Section 5.

The estimated ground water level (GWL) from the CPT GEF file was used to compute the initial porewater pressure ( $u_0$ ). As an alternative it can be defined by the user. In this study, the GWL is set to 1 m below the ground. Based on the estimated unit weight and porewater pressure distribution, total and effective stresses are calculated over depth. In addition, normalized CPT parameters are assessed as follows:

- Normalized cone resistance

$$Q_t = \frac{q_t - \sigma_v}{\sigma'_v} \quad (4)$$

- Normalized porewater pressure

$$B_q = \frac{(u_2 - u_0)}{(q_t - \sigma_v)} \quad (5)$$

- Normalized cone parameter with variable stress exponent  $n$  that varies with soil behaviour type index ( $I_c$ ) and calculated in an iterative process as follows:

$$Q_{tn} = \frac{q_t - \sigma_v}{p_a} / \left( \frac{p_a}{\sigma'_v} \right)^n \quad (6)$$

$$n = 0.381(I_c) + 0.05 \left( \frac{\sigma'_v}{p_a} \right) - 0.15 \leq 1.0 \quad (7)$$

$$I_c = \sqrt{(3.47 - \log Q_{tn})^2 + (\log F_r + 1.22)^2} \quad (8)$$

The initial parameters do not need to be defined in the methods CSV file. They are calculated internally and act as source parameters for the graph (Fig. 3).

##### 4.2. Stress history

The stress history is often defined based on the overconsolidation ratio,  $OCR = \sigma'_p / \sigma'_v$ , where  $\sigma'_p$  is the preconsolidation stress. In the present study, the following three approaches are used to determine OCR:

$$OCR = \frac{\sigma'_p}{\sigma'_v} = \frac{0.33(q_t - \sigma_v)^{m'}}{\sigma'_v} \quad (9)$$

by (Mayne et al. 2009), where  $m'$  is the yield stress exponent that increases with fine content and decreases with mean grain size. Mayne (2017) proposed determining  $m'$  from  $I_c$  (Eq. 8) as follows:

$$m' = 1 - \frac{0.28}{1 + \left(\frac{I_c}{2.65}\right)^{25}} \quad (10)$$

$$OCR = 1.026 B_q^{-1.077} \quad (11)$$

by (D'Ignazio et al. 2019).

$$OCR = 0.63 B_q^{-1.286} \quad (12)$$

by (Schroeder, K. H. Andersen, and Tjok 2006).

### 4.3. Strength parameters

The undrained shear strength ( $s_u$ ) could be determined from CPT results as follows:

$$s_u = \frac{q_t - \sigma_v}{N_{kt}} \quad (13)$$

$$s_u = \frac{u_2 - u_0}{N_{\Delta u}} \quad (14)$$

$$s_u = \frac{q_t - u_2}{N_{ke}} \quad (15)$$

Where  $N_{kt}$ ,  $N_{\Delta u}$  and  $N_{ke}$  are bearing factors for net tip resistance, excess porewater pressures and effective cone resistance respectively. Average initial values for these factors could be selected as, 12, 6 and 8 for  $N_{kt}$ ,  $N_{\Delta u}$  and  $N_{ke}$  respectively (Mayne 2016).

### 4.4. Shear wave velocity

The shear wave velocity ( $V_s$ ) is used to determine the small-strain shear modulus ( $G_0$ ). The following 3 methods are used to determine  $V_s$ :

$$V_s = (10.1 \log q_c - 11.4)^{1.67} (f_s/q_c \times 100)^{0.3} \quad (16)$$

by (Hegazy and Mayne 1995).

$$V_s = [\alpha_{vs}(q_t - \sigma_v)/p_a]^{0.5} \quad (17)$$

by (Robertson 2015), where  $\alpha_{vs} = 10^{(0.55I_c + 1.68)}$ .

$$V_s = 0.831 Q_{tn} \left(\frac{\sigma'_p}{p_a}\right)^{0.25} e^{1.786I_c} \quad (18)$$

by (Hegazy and Mayne 2006).

### 4.5. Stiffness parameters

$G_0$  is determined from  $V_s$  as follows:

$$G_0 = \rho V_s^2 \quad (19)$$

where  $\rho$  is the density of the soil. As an alternative, the tip resistance can be used to estimate  $G_0$  according to Eq. 20 and 21.

$$G_0 = 2.78 q_c^{1.335} \quad (20)$$

by (Mayne and Rix 1993).

$$G_0 = 50(q_t - \sigma_v)^{m^*} \quad (21)$$

by (Mayne 2007), where  $m^*=0.6$  for clean quartz sands, 0.8 for silts and 1.0 for intact clays of low to medium sensitivity.

The 1-D constrained tangent modulus,  $M$  is used to predict settlements. The following method by (Robertson 2009) is used:

$$M = \alpha_M(q_t - \sigma_v) \quad (22)$$

Robertson (2009) suggested a procedure to determine  $\alpha_M$  based on  $I_c$  (Eq. 8) as follows:

- For  $I_c > 2.2$ 
  - $\alpha_M = Q_{tn}$  (if  $Q_{tn} < 14$ )
  - $\alpha_M = 14$  (if  $Q_{tn} > 14$ )
- For  $I_c < 2.2$ 
  - $\alpha_M = 0.03[10^{(0.55I_c + 1.68)}]$

The methods illustrated in the previous subsections were used to determine soil parameters for CPTu 2 and CPTu 18 (Fig. 1). In the present study CPTu results were averaged every 1 m and these averaged values were used in module 2 (Fig. 2). If the layers are determined manually, the SBT for each layer must be provided by the user. This SBT will act as a validity criterion for the methods CSV file. In this study, as the test site is a homogenous soft clay deposit, all the layers had SBT(3) corresponding to clay according to Robertson (2010) (Table 2). Fig. 4 presents the generated graph for layer 5 (from 6 m to 7 m) for CPTu 18. The averaging process resulted in 20 and 18 layers for CPTu 2 and CPTu 18, respectively.

## 5. Results

The results of different in-situ correlations are compared for CPTu 2 and CPTu 18 with laboratory results in Figs. 5-6. Figs. 5.a, 5.c, 5.e, 6.a, 6.c, 6.e show the results for CPTu 18 (area SEC), while Figs. 5.b, 5.d, 5.f, 6.b, 6.d, 6.f indicate the results for CPTu 2 (area SC). The black dotted, horizontal lines indicate the respective unit boundaries.

The total unit weight was assessed from direct measurements and based on measured water contents (Gundersen et al. 2019). Figs. 5.a-b show that Eqs. (1 & 3) underestimate the laboratory results. However, Eq. (2) results in a reasonable agreement with laboratory results. For this reason, Eq. (2) was selected for computing the initial unit weight which was used to assess the total and effective stress.

OCR was assessed from oedometer tests (either from incremental loading (IL) tests or from constant rate of strain (CRS) tests). The tested samples were obtained from block samples and tube samples. The assessment of sample quality was performed according to Lunne, Berre, and Strandvik (1997). As described in more detail by Gundersen et al. (2019) samples of quality class 1 and 2 are considered for discussion.

In Figs. 5.c-d results of Eqs. (9-12) are compared with oedometer results. It should be noted that in Fig. 5.c, all samples were added to the figure irrespective of their sample quality as there were only two soil specimens of high quality (at area SEC).

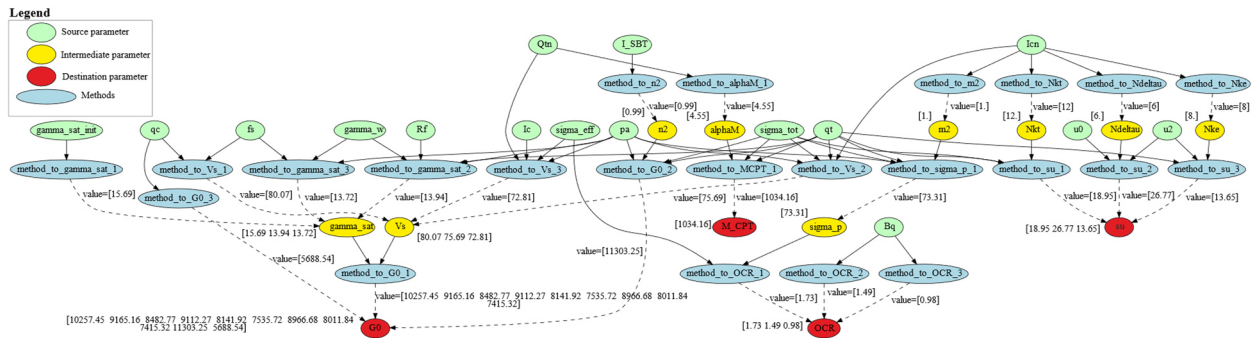


Figure 4. Generated graph for layer 5 (6 m to 7 m below the ground surface) for CPTu 18.

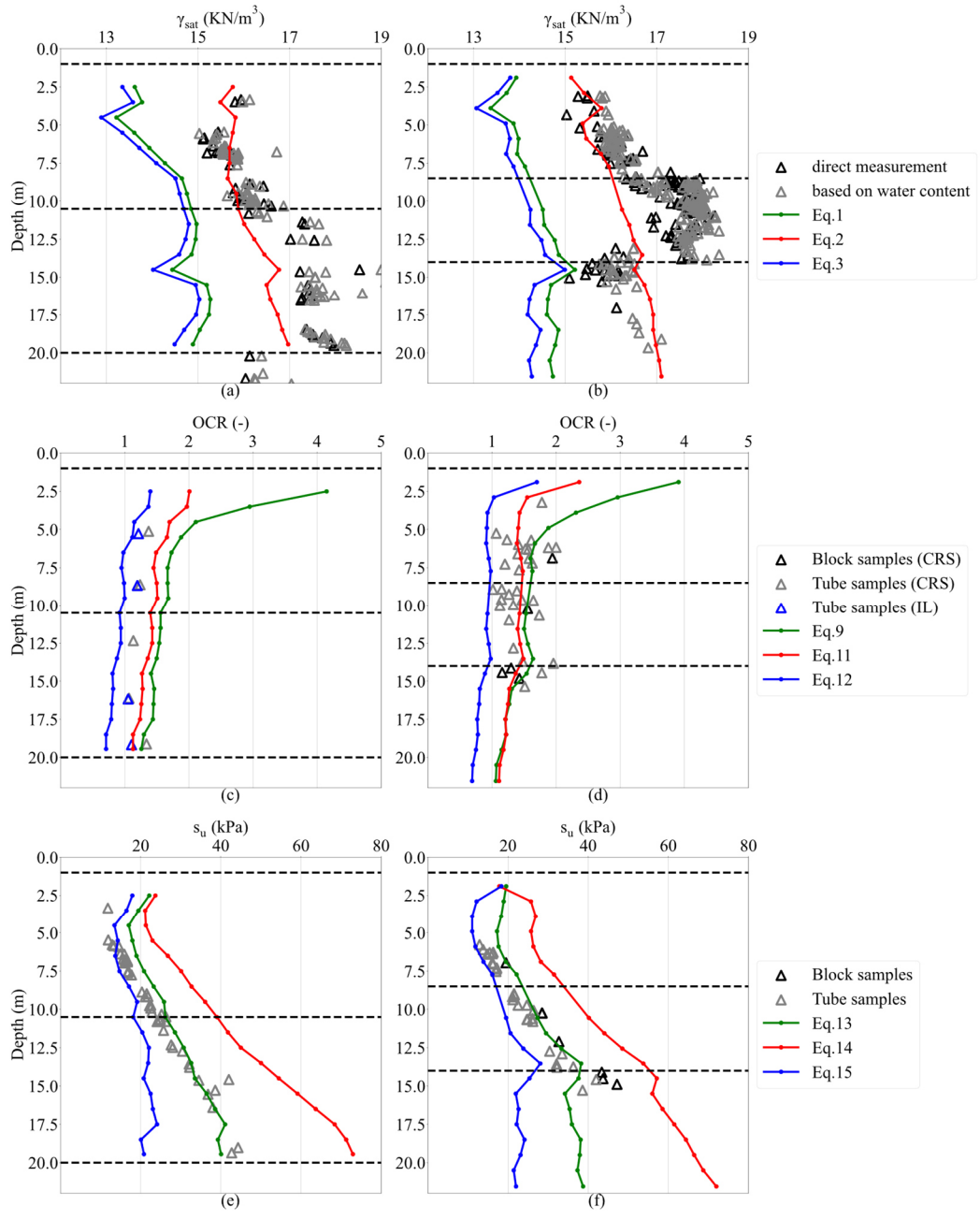
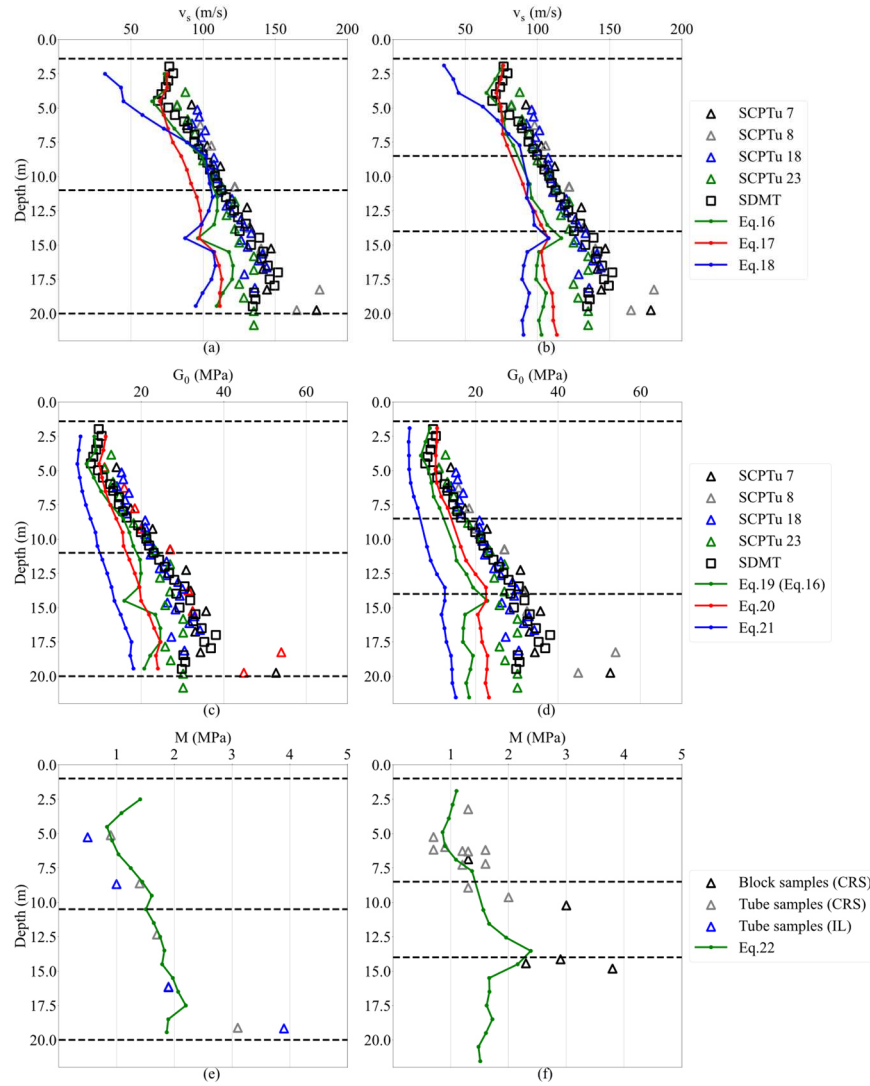


Figure 5. Comparison between APD and interpreted values at Onsøy soft clay test site (a), (c) and (e) present results for CPTu 18, while (b), (d) and (f) present results for CPTu 2.



**Figure 6.** Comparison between APD and interpreted values at Onsøy soft clay test site (a), (c) and (e) present results for CPTu 18, while (b), (d) and (f) present results for CPTu 2.

Reference values for  $s_u$  were derived using triaxial compression test results.  $s_u$  determined from block samples are around 5-15 % higher than the ones obtained from tube samples (Gundersen et al. 2019). A comparison between the output of Eqs. (13-15) and laboratory results is shown in Figs. 5.e-f. The 3 equations bound the laboratory results. Eq. 14 provides an upper bound, Eq. 15 a lower bound and Eq. 13 is situated in between leading to the best agreement with laboratory data.

The shear wave velocity obtained from SCPT 7, 8, 18 and 23 (ONSC 7, 8, 18 & 23 in the database) and SDMT are compared with estimated values from Eqs. (16-18) (see Figs. 6.a-b). The four seismic CPT and SDMT were executed in area SEC.  $V_s$  obtained from these tests were added to Fig. 6.b (representing area SC) as no  $V_s$  is available there.

Similar to  $V_s$ ,  $G_0$  is presented in Figs. 6.c-d.  $G_0$  is derived from bulk density and shear wave velocity according to Eq. (19). The reference values, indicated by triangular and square symbols, were calculated based on in-situ shear wave velocity measurements. Eq. (20) and Eq. (21), which estimates  $G_0$  based on  $q_t$  or  $q_c$

underestimate  $G_0$  significantly. Focusing on  $G_0$  obtained from in-situ measurements, all Eqs. underestimate  $G_0$ , specially in Units III and IV. In Unit II, a reasonable fit is obtained. These results indicate that correlations used to obtain  $G_0$  and  $V_s$  require further investigation.

The constrained modulus was determined based on Janbu modulus concept (Gundersen et al. 2019). The results of Figs. 6.e-f indicate a good agreement between in-situ (Eq. (22)) and laboratory results at shallow depths. However, at deeper depths, values obtained from Eq. (22) underestimate the constrained modulus.

## 6. Conclusions

In the present paper, soil parameters were derived from cone penetration tests using the APD (Automated Parameter Determination) approach. Results of existing correlations were compared with laboratory results at Onsøy soft clay test site (NGTS). This comparison helped to validate individual correlations and to update the compiled methods database.

Fig. 4. presents an example of a generated graph using a selected (limited) number of methods. The fact that several methods exist to compute the same parameter,



leads to a scatter in the obtained values. As shown in Figs. 5-6, some methods perform better than others. In case all methods (in the database) are used, the scatter is even more. Dealing with this scatter and selecting a suitable approach for choosing a specific value from the range of the computed values is part of ongoing research.

The transition from soil parameters to constitutive model parameters was not discussed in this contribution. The current database already consists of several correlations between soil parameters and input parameters for the Hardening Soil Small Model (HSsmall) (Benz 2007). This transition is considered as one of the key aspects of the research project.

The presented framework is characterized by two key features, transparency and adaptability. The knowledge and experience of the users can be incorporated in the system by altering the provided database. The research project aims to increase the confidence in deriving soil parameters based on in-situ tests. The expansion of the current framework to accommodate additional in-situ tests is currently in progress. Recently, DMT was added to the framework and the system successfully imported DMT results and generated graphs with intermediate and destination parameters for several layers. The validation of this expansion is currently under investigation.

## References

- Benz, T. 2007. "Small-Strain Stiffness of Soils and Its Numerical Consequences." Ph.D. thesis, University of Stuttgart.
- Brinkgreve, R.B.J. 2019. "Automated Model and Parameter Selection: Incorporating Expert Input into Geotechnical Analyses." *Geostrata* 23 (1): 38–45. doi:10.1061/geosek.0000115.
- D'Ignazio, M., T. Lunne, K. H. Andersen, S. Yang, B. Di Buò, and T. Lämsivaara. 2019. "Estimation of Preconsolidation Stress of Clays from Piezocone by Means of High-Quality Calibration Data." *AIMS Geosciences* 5 (2): 104–16. doi:10.3934/geosci.2019.2.104.
- Doherty, J. P., S. Gourvenec, F. M. Gaone, J. A. Pineda, R. Kelly, C. D. O'Loughlin, M. J. Cassidy, and S. W. Sloan. 2018. "A Novel Web Based Application for Storing, Managing and Sharing Geotechnical Data, Illustrated Using the National Soft Soil Field Testing Facility in Ballina, Australia." *Computers and Geotechnics* 93:3–8. doi:10.1016/j.compgeo.2017.05.007.
- Gundersen, A. S., R. C. Hansen, T. Lunne, J. S. L'Heureux, and S. O. Strandvik. 2019. "Characterization and Engineering Properties of the NGTS Onsøy Soft Clay Site." *AIMS Geosciences* 5 (3): 665–703. doi:10.3934/geosci.2019.3.665.
- Hegazy, Y. A., and P. Mayne. 1995. "Statistical Correlations Between Vs and CPT Data for Different Soil Types."
- Hegazy, Y. A., and P. Mayne. 2006. "A Global Statistical Correlation Between Shear Wave Velocity and Cone Penetration Data." 243–48. doi:10.1061/40861(193)31.
- Jaky, J. 1944. "The Coefficient of Earth Pressure at Rest." *J. of the Society of Hungarian Architects and Engineers*, 355–58. <https://cir.nii.ac.jp/erid/1571698599493336320>.
- Kulhawy, F. H., and P. Mayne. 1990. "Manual on Estimating Soil Properties for Foundation Design."
- L'Heureux, J. S., and T. Lunne. 2020. "Characterization and Engineering Properties of Natural Soils Used for Geotesting." *AIMS Geosciences* 6 (1): 35–53. doi:10.3934/geosci.2020004.
- Lengkeek, H. J., J. de Greef, and S. Joosten. 2018. "CPT Based Unit Weight Estimation Extended to Soft Organic Soils and Peat." In *Cone Penetration Testing IV: Proceedings of the 4th International Symposium on Cone Penetration Testing (CPT 2018), June 21-22, 2018, Delft, the Netherlands*.
- Lunne, T., T. Berre, and S. Strandvik. 1997. "Sample Disturbance Effects in Soft Low Plastic Norwegian Clay." *Symposium on Recent Developments in Soil and Pavement Mechanics, Rio de Janeiro, Brazil*. <https://trid.trb.org/view/476476>.
- Lunne, T., P. K. Robertson, and J. J. M. Powell. 1997. *Cone Penetration Testing in Geotechnical Practice*. First edition. Boca Raton, FL: CRC Press.
- Marzouk, I., F. Tschuchnigg, F. Paduli, H. J. Lengkeek, and R.B.J. Brinkgreve. "Determination of Fine-Grained Soil Parameters Using an Automated System." In *Cone Penetration Testing 2022*, 540–45.
- Mayne, P. 2007. "In-Situ Test Calibrations for Evaluating Soil Parameters." In *Characterisation and engineering properties of natural soils*.
- Mayne, P. 2014. "Interpretation of Geotechnical Parameters from Seismic Piezocone Tests."
- Mayne, P. 2016. "Evaluating Effective Stress Parameters and Undrained Shear Strengths of Soft-Firm Clays from CPTu and DMT." Fifth International Conference on Geotechnical and Geophysical Site Characterization (ISC'5).
- Mayne, P. 2017. "Stress History of Soils from Cone Penetration Tests." *Soils and Rocks* (3).
- Mayne, P., M. Coop, S. Springman, A. B. Huang, and J. Zornberg. 2009. "State-of-the-Art Paper (SOA-1): Geomaterial Behavior and Testing."
- Mayne, P., and G. J. Rix. 1993. "Gmax-Qc Relationships for Clays." *Geotech. Test. J.* 16 (1): 54. doi:10.1520/GTJ10267J.
- Norwegian Geotechnical Institute. 2019. "Norwegian GeoTest Sites—Field and Laboratory Test Results from NGTS Soft Clay Site—Onsøy: Report No. 20160154-10-R. Rev. 2."
- Robertson, P. K. 2009. "Interpretation of Cone Penetration Tests — A Unified Approach." *Can. Geotech. J.* 46 (11): 1337–55. doi:10.1139/T09-065.
- Robertson, P. K. 2010. "Soil Behaviour Type from the CPT: An Update." 2nd International Symposium on Cone Penetration Testing, Huntington Beach 2, 575–83.
- Robertson, P. K. 2015. "Guide to Cone Penetration Testing for Geotechnical Engineering." Proceedings of the 3rd International Symposium on Cone Penetration Testing (CPT14, Las Vegas).
- Robertson, P. K. 2016. "Cone Penetration Test (CPT)-Based Soil Behaviour Type (SBT) Classification System — An Update." *Can. Geotech. J.* 53 (12): 1910–27. doi:10.1139/cgj-2016-0044.
- Robertson, P. K., and K. L. Cabal. 2010. "Estimating Soil Unit Weight from CPT." <https://www.cpt-robertson.com/PublicationsPDF/Unit%20Weight%20Rob%20%26%20Cabal%20CPT10.pdf>.
- Schroeder, K., K. H. Andersen, and K. M. Tjok. 2006. "Laboratory Testing and Detailed Geotechnical Design of the Mad Dog Anchors." OnePetro.
- van Berkom, I.E., R.B.J. Brinkgreve, H. J. Lengkeek, and A. K. de Jong. 2022. "An Automated System to Determine Constitutive Model Parameters from in Situ Tests." *Proceedings of the 20th International Conference on Soil Mechanics and Geotechnical Engineering, Sydney 2021*.